Chapter 4

Peristaltic Transport of Herschel-Bulkley Fluids in Tubes of Variable Cross Section Induced by Dilating Peristaltic Waves: Application to sliding hiatus hernia

4.1 Introduction

The dome shaped muscle which separates the abdomen from the chest is called diaphragm. The oesophagus passes through an opening, called hiatus, in the diaphragm to connect to the stomach. Bulging up of the abdominal cavity through the oesophageal hiatus into the part of the thoracic cavity between the lungs is called hiatus hernia (Fig. 4.1). One of the recognized theories of origin of this hiatus hernia is that intra-abdominal pressure increases above the normal value to rise the normal gradient between intra-thoracic and intra-abdominal pressure. Consequently, the oesophago-gastric junction is pushed up into hiatus (Christensen and Miftakhov, 2000). Due to this herniation oesophagus diverges at the distal end or is a combination of divergence and convergence. This model investigates the effect of this non-uniformity of oesophagus on swallowing of such food stuffs which possess Herschel-Bulkley fluid nature.

There are cases of malfunctioning of oesophagus such as hiatus hernia, achalasia etc. (Kahrilas et al., 1999; Carlson et al., 2018). We focus our study on sliding hiatus hernia which is very common and is defined as a significant axial prolapse of a portion of the stomach through the diaphragmatic oesophageal hiatus. It is usually described as a more than 2 cm

The contents of this chapter are published in Int. J. Dyn. Control (2018), doi: org/10.1007/s40435-018-0454-7.

separation of the upward displaced oesophago-gastric junction and diaphragmatic impression (Weyenberg, 2013).

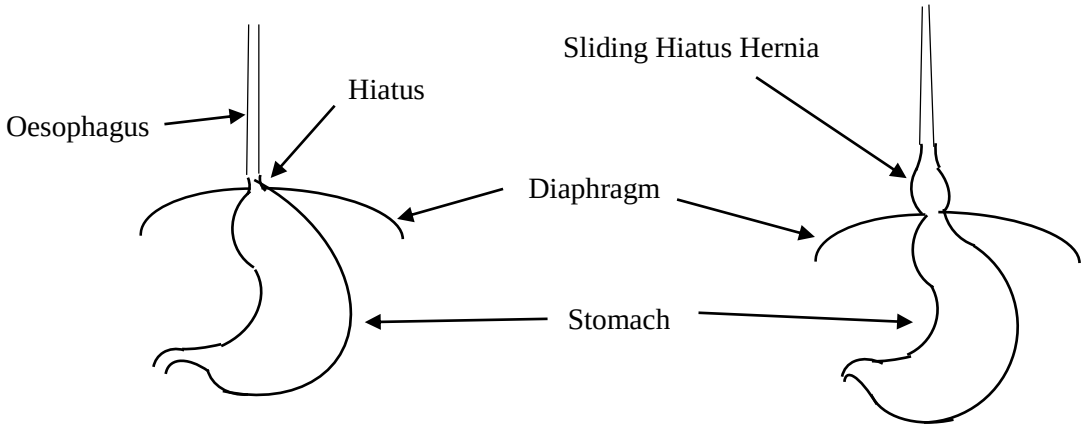

Fig. 4.1(a-b) *Schematic diagrams for* (a) *Normal oesophagus and* (b) *Sliding hiatus hernia affected oesophagus*

The lower oesophageal sphincter is a thickened area of the circular muscle layer of the distal oesophagus, in humans extending over an axial length of 2–4 cm. The main function of the lower oesophageal sphincter is to generate a high-pressure zone to save from harm the oesophagus against reflux from caustic gastric contents. During swallowing or belching, its muscle must relax temporarily in order to permit passage of ingested food or intra-gastric air. Swallow-induced relaxation is part of primary peristalsis (Boeckxstaens, 2005).

Herschel-Bulkley fluids are general class of non-Newtonian fluids that possess a yield stress when the local shear is below a certain limit. When the yield stress exceeds this limit, the fluid flows with a non-linear stress-strain relationship as a shear-thickening or a shear thinning fluid. Some edible semi-fluids such as tomato puri, melted chocolate (Bingham fluid), peanut butter, ketchup (pseudo plastic) and cornstarch in water (dilatant) are special cases of Hurschel-Bulkley fluid (Bourne, 2002).

Study of the mechanism of peristalsis, in mechanical and physiological situation, has been the object of scientific research for long. Since the first investigation of Latham (1966),

several theoretical and experimental attempts have been made to understand peristaltic action in different situations. In the early studies of peristalsis most of the theoretical investigations and clinical observations took time to gain momentum (Latham, 1966; Fung and Yih, 1968; Shapiro et al., 1969). These investigations were carried out by considering fluid as Newtonian flowing in a tube or channel having uniform cross sectional area. With the development of medical and physical sciences, it has been recognized that the bio-fluids do not, in general, behave like Newtonian fluids and hence such a consideration does not appropriately model flows in small blood vessels, intestine, the cervical canal etc. It has now been accepted that most of the physiological fluids behave like non-Newtonian fluids. Peristalsis in male reproductive system was observed experimentally and numerically by Batra (1974), Guha et al. (1975), Gupta and Seshadri (1976) and Srivastava and Srivastava (1985). Guha et al. (1975) studied the transport of the spermatic fluid in the vas deferens of monkey and reported that the transportation during ejaculation is mainly due to contraction of the ampulla and filling during the non-ejaculatory phase is due to peristalsis and epididymal pressure. Srivastava and Srivastava (1984) modelled peristaltic flows of Casson fluids (blood) flowing inside small capillaries and blood vessels. Srivastava and Srivastava (1985) examined peristaltic flows of power law fluids in the vas deference by considering it a non-uniform diverging tube. Misra and Pandey (1995) modeled axisymmetric peristaltic motion of a Newtonian viscous incompressible fluid through a flexible tube of changing cross section, where the nonlinear convective acceleration terms were considered non-negligible compared to the viscous terms. Their reports were more ascribable than the previous reports for spermatic flow reported by Guha et al. (1975). Eytan and Elad (1999) and Eytan et al. (2001) investigated the effect of peristalsis in embryo transport within the uterine cavity. They discussed in detail the phenomenon of trapping and how the particle reflux impedes the embryo implantation at the fundus. Hariharan et al. (2008) studied peristaltic transport of non-Newtonian fluid in a diverging tube with different waveforms and concluded that square wave has the best pumping characteristics of all the wave forms while the triangular wave has the worst characteristics. Among the most recent literature, Prakash and Tripathi (2018) used the same type of linear tapering.

Li and Brasseur (1993) studied the transport of food bolus in the oesophagus with integral and non- integral number of waves. Misra and pandey (2001) gave a more suitable

model with modified wall equation for oesophageal swallowing. Pandey and Chaube (2010; 2011b) investigated the peristaltic transport of Maxwell and viscoelastic fluid in a tube and a channel of varying cross sections respectively. Kahrilas et al. (1995) reported an experimental investigation of high pressure zone located in the lower part of the oesophagus whose length varies from a normal oesophagus to an oesophagus which suffers from hiatus hernia. In another experimental investigation, Xia et al. (2009) measured oesophageal wall thickness in contracted and dilated states through CT images of adult patients without oesophageal diseases. On the basis of this, Pandey et al. (2017) concluded that in the dilated state the upper oesophagus is thicker while in the contracted state the lower oesophagus is thicker and modeled the oesophageal swallowing with peristaltic waves of exponentially increasing wave amplitude for Newtonian fluid. Several reports are available that explain the mathematics of peristalsis and its effect on flow in a diverging tube with non-Newtonian fluid. Due to sliding hiatus hernia the cross sectional area of the oesophagus does not remain uniform throughout its length, and consequently, it gets diverged at the distal end. Sometimes it may be divergent and then convergent near the distal end. In light of this, purpose of present analysis is to study the effect of sliding hiatus hernia on the oesophageal swallowing with dilating peristaltic wave amplitude for non-Newtonian fluid (Herschel-Bulkley fluid).

The various assumptions including the types of the fluid and the motion considered, the wall equation etc. and the mathematical formulation of the model are presented in Section 4.2. Section 3 deals with the method of solution for deducing velocities and the axial pressure. Numerical results and discussions including physical interpretations are given in Section 4.4 which is followed by conclusions drawn and described in Section 4.5.

4.2 Mathematical formulation

We consider oesophagus as a circular cylindrical tube of finite length whose cross sectional area varies due to hiatus hernia. Progressive sinusoidal wave trains with dilating amplitude propagate along the oesophageal wall of the tube. Therefore, wall equation given by Pandey et al. (2017) gets modified for the diverging tube, which for the single wave propagation may be given by

$$H'(x',t',k') = \begin{cases} a + b'x' - \emptyset' e^{k'x'} cos^2 \frac{\pi}{\lambda}(x' - ct'), & \text{during } \left[t', \quad t' + \lambda/c\right], \\ a + b'x' - \emptyset' e^{k'x'}, & \text{otherwise} \end{cases} \tag{4.1}$$

where $H', x', k', t', a, b', \emptyset', \lambda, l'$ and c respectively denote radial displacement of the wall from the centre line, axial coordinate, dilation parameter, time parameter, radius of the tube at inlet, slop of tube wall, amplitude of the wave, wavelength , length of tube and wave velocity (Fig. 4.2).

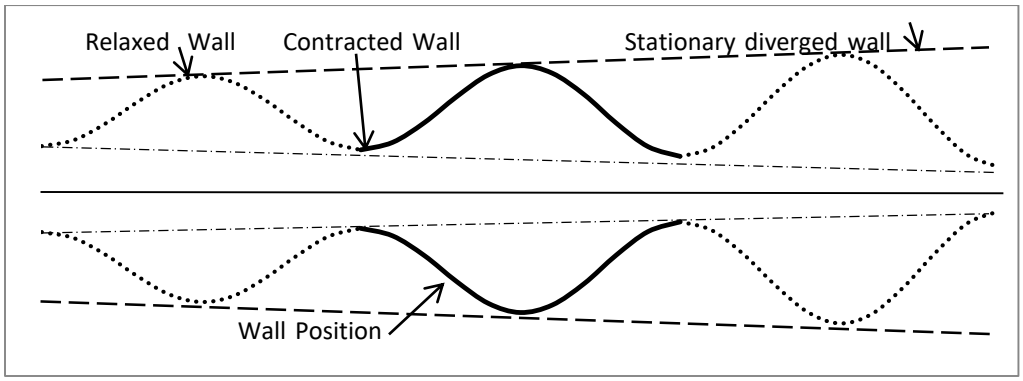

Fig. 4.2 *Schematic diagram of the flow under peristaltic waves of progressively dilating amplitude. Converging dashed dotted lines touching contracted wall positions indicate that the wave-amplitude dilates. Diverging dashed lines touching relaxed wall indicate stationary wall. The continuous solid wave indicates that at a time only single bolus will be transported; similar boluses lagging behind or leading simply symbolize that the previous position and the future position of the bolus.*

The continuity and Navier-Stokes equations for the axi-symmetric unsteady flow of a viscous non-Newtonian incompressible fluid with no body forces are given by

$$\frac{\partial u'}{\partial x'} + \frac{1}{r'}\frac{\partial (r'v')}{\partial r'} = 0. \tag{4.2}$$

$$\rho\left(\frac{\partial}{\partial t'} + u'\frac{\partial}{\partial x'} + v'\frac{\partial}{\partial r'}\right)u' = -\frac{\partial p'}{\partial x'} + \frac{1}{r'}\frac{\partial (r'\tau'_{r'x'})}{\partial r'} + \frac{\partial \tau'_{x'x'}}{\partial x'}, \tag{4.3}$$

$$\rho\left(\frac{\partial}{\partial t'} + u'\frac{\partial}{\partial x'} + v'\frac{\partial}{\partial r'}\right)v' = -\frac{\partial p'}{\partial r'} + \frac{1}{r'}\frac{\partial (r'\tau'_{r'r'})}{\partial r'} + \frac{\partial \tau'_{x'r'}}{\partial x'} - \frac{\tau'_{\theta'\theta'}}{r'}. \tag{4.4}$$

The Herschel-Bulkley fluid model is represented as

$$\left.\begin{aligned} \tau'_{r'x'} &= m\left|\frac{\partial u'}{\partial r'}\right|^{n-1}\frac{\partial u'}{\partial r'} + \tau'_0, && \tau'_{r'x'} > \tau'_0 \\ \frac{\partial u'}{\partial r'} &= 0, && \tau'_{r'x'} \le \tau'_0 \end{aligned}\right\}, \tag{4.5}$$

where $\tau'_{ij}(i, j = r', x', \theta'), \tau'_0, m, n, \rho, p', u', v'$ and r' are the shear stress components, yield stress, flow consistency index, flow behavior index, fluid density, pressure, axial velocity,

radial velocity and radial coordinate respectively. The effective viscosity, in Herschel-Bulkley fluid model, is defined as $m\left|\frac{\partial u'}{\partial r'}\right|^{n-1}$. Since we plan to apply long wavelength approximation, stress components other than this will get eliminated, for that reason, the rest are not defined here.

The non-dimensionalisation of various parameters for dimensional similarity is done as follows:

$$\left.\begin{aligned} x = \frac{x'}{\lambda},\ r = \frac{r'}{a},\ t = \frac{ct'}{\lambda},\ u = \frac{u'}{c},\ v = \frac{v'}{c\alpha},\ \alpha = \frac{a}{\lambda},\ H = \frac{H'}{a}, \\ k = k'\lambda,\ \tau_0 = \frac{\tau'_0}{m}\left(\frac{a}{c}\right)^n,\ \tau_{ij} = \frac{\tau'_{i'j'}}{m}\left(\frac{a}{c}\right)^n (i,j = r,x,\ \theta),\ l = \frac{l'}{\lambda}, \\ \phi = \frac{\emptyset'}{a},\quad p = \frac{p'a^2}{mc\lambda},\quad Q = \frac{Q'}{\pi a^2 c},\quad R_e = \frac{\rho c^{2-n} a^n \alpha}{m},\quad b = \frac{b'\lambda}{a}, \end{aligned}\right\} \tag{4.6}$$

where Q, α and R_e are volume flow rate, wave number and Reynolds number respectively.

Using the above defined dimensionless parameters in Eqs.(4.1)-(4.5) and applying low Reynolds number and long wavelength approximations, Eqs.(4.1)-(4.5) reduce respectively to the following dimensionless form

$$H(x,t,k) = \begin{cases} 1 + bx - \emptyset e^{kx} cos^2\pi(x-t), & \text{during } [t,\ \ t+1] \\ 1 + bx - \emptyset e^{kx}, & \text{otherwise} \end{cases}, \tag{4.7}$$

$$\frac{\partial u}{\partial x} + \frac{1}{r}\frac{\partial (rv)}{\partial r} = 0, \tag{4.8}$$

$$\frac{\partial p}{\partial x} = \frac{1}{r}\frac{\partial (r\tau_{rx})}{\partial r}, \tag{4.9}$$

$$\frac{\partial p}{\partial r} = 0, \tag{4.10}$$

$$\left.\begin{aligned} \tau_{rx} &= \left|\frac{\partial u}{\partial r}\right|^{n-1}\frac{\partial u}{\partial r} + \tau_0, && \tau_{rx} > \tau_0 \\ \frac{\partial u}{\partial r} &= 0, && \tau_{rx} \le \tau_0 \end{aligned}\right\}. \tag{4.11}$$

The following boundary conditions, given in dimensionless form, are imposed on the governing equations:

$$u(r,x,t)|_{r=H} = 0,\ v(r,x,t)|_{r=H} = \frac{\partial H}{\partial t},\ \ v(r,x,t)|_{r=H_{pl}} = 0,\quad \left.\frac{\partial u}{\partial r}\right|_{r=H_{pl}} = 0. \tag{4.12}$$

where H_{pl} is the radius of the plug flow region, and it is defined by

$$H_{pl} = \frac{2\tau_0}{\frac{\partial p}{\partial x}}. \tag{4.13}$$

4.3 Solution

The integration of Eq. (4.9) with respect to r, in view of Eq. (4.10), gives

$$\tau_{rx} = \frac{r}{2}\frac{\partial p}{\partial x} + \frac{C(x,t)}{2}, \tag{4.14}$$

where $C(x,t)$ is an arbitrary function of x and t.

Using Eq. (4.11) in (4.14) and then applying fourth boundary condition of Eq. (4.12) with (4.13), we get

$$\frac{\partial u}{\partial r} = \left(\frac{r}{2}\frac{\partial p}{\partial x} - \tau_0\right)^{\frac{1}{n}}.$$

Again integrating it with respect to r and applying first boundary condition of Eq. (4.12), the axial velocity may be, in view of Eq. (4.7), given by

$$u(x,r,t) = \frac{\frac{\partial p}{\partial x}\left|\frac{\partial p}{\partial x}\right|^{\left(\frac{1}{n}-1\right)}}{2^{\frac{1}{n}}\left(1+\frac{1}{n}\right)}\left[\{r - H_{pl}\}^{\left(1+\frac{1}{n}\right)} - \{1 + bx - \emptyset\, e^{kx}cos^2\pi(x-t) - H_{pl}\}^{\left(1+\frac{1}{n}\right)}\right] \tag{4.15}$$

On putting $r = H_{pl}$ in Eq. (4.15), the plug flow velocity is derived as

$$u_{pl}(x,t) = -\frac{\frac{\partial p}{\partial x}\left|\frac{\partial p}{\partial x}\right|^{\left(\frac{1}{n}-1\right)}}{2^{\frac{1}{n}}\left(1+\frac{1}{n}\right)}\{1 + bx - \emptyset\, e^{kx}cos^2\pi(x-t) - H_{pl}\}^{\left(1+\frac{1}{n}\right)}. \tag{4.16}$$

Introducing the axial velocity given in Eq. (4.15), into continuity equation (4.8) and solving it together with third boundary condition of Eq. (4.12) and then dividing resulting equation by r, we obtain the radial velocity as

$$v(x,r,t) = \frac{\left|\frac{\partial p}{\partial x}\right|^{\left(\frac{1}{n}-1\right)}\frac{\partial p}{\partial x}\{1+bx-\emptyset\, e^{kx}cos^2\pi(x-t)-H_{pl}\}^{\frac{1}{n}}\{b+\pi\emptyset\, e^{kx}\sin 2\pi(x-t)-\emptyset\, ke^{kx}cos^2\pi(x-t)\}r}{2^{\left(1+\frac{1}{n}\right)}}$$

$$+\frac{\frac{1}{n}\left|\frac{\partial p}{\partial x}\right|^{\left(\frac{1}{n}-2\right)}\frac{\partial p\partial^2 p}{\partial x\partial x^2}\{1+bx-\emptyset\, e^{kx}cos^2\pi(x-t)-H_{pl}\}^{\left(1+\frac{1}{n}\right)}r}{2^{\left(1+\frac{1}{n}\right)}\left(1+\frac{1}{n}\right)}-\frac{\frac{1}{n}\left|\frac{\partial p}{\partial x}\right|^{\left(\frac{1}{n}-2\right)}\frac{\partial p\partial^2 p}{\partial x\partial x^2}\{r-H_{pl}\}^{\left(2+\frac{1}{n}\right)}}{2^{\frac{1}{n}}\left(1+\frac{1}{n}\right)\left(2+\frac{1}{n}\right)}$$

$$+\frac{\frac{1}{n}\left|\frac{\partial p}{\partial x}\right|^{\left(\frac{1}{n}-2\right)}\frac{\partial p\partial^2 p}{\partial x\partial x^2}\{1+bx-\emptyset\, e^{kx}cos^2\pi(x-t)-H_{pl}\}^{\left(3+\frac{1}{n}\right)}}{2^{\frac{1}{n}}\left(1+\frac{1}{n}\right)\left(2+\frac{1}{n}\right)\left(3+\frac{1}{n}\right)r}-\frac{\frac{1}{n}\left|\frac{\partial p}{\partial x}\right|^{\left(\frac{1}{n}-2\right)}\frac{\partial p\partial^2 p}{\partial x\partial x^2}\{1+bx-\emptyset\, e^{kx}cos^2\pi(x-t)-H_{pl}\}^{\left(1+\frac{1}{n}\right)}H_{pl}^2}{2^{\left(1+\frac{1}{n}\right)}\left(1+\frac{1}{n}\right)}$$

$$-\frac{\left|\frac{\partial p}{\partial x}\right|^{\left(\frac{1}{n}-1\right)}\frac{\partial p}{\partial x}\{1-\emptyset\, e^{kx}cos^2\pi(x-t)-H_{pl}\}^{\frac{1}{n}}\{b+\pi\emptyset\, e^{kx}\sin 2\pi(x-t)-\emptyset\, ke^{kx}cos^2\pi(x-t)\}H_{pl}^2}{2^{\left(1+\frac{1}{n}\right)}r}. \quad (4.17)$$

Now applying the second boundary condition of Eq. (4.12) in Eq. (4.17), and simplifying, we get

$$H\frac{\partial H}{\partial t}=\frac{1}{n}\frac{\partial p}{\partial x}\left|\frac{\partial p}{\partial x}\right|^{\left(\frac{1}{n}-2\right)}\frac{\partial^2 p}{\partial x^2}S+\left|\frac{\partial p}{\partial x}\right|^{\left(\frac{1}{n}-1\right)}\frac{\partial p}{\partial x}T\,, \quad (4.18)$$

where

$$S=\frac{\{1+bx-\emptyset e^{kx}cos^2\pi(x-t)-H_{pl}\}^{\left(1+\frac{1}{n}\right)}\left\{1-2\emptyset e^{kx}cos^2\pi(x-t)+\emptyset^2e^{2kx}cos^4\pi(x-t)+b^2x^2+2bx-2bx\emptyset e^{kx}cos^2\pi(x-t)\right\}}{2^{\left(1+\frac{1}{n}\right)}\left(1+\frac{1}{n}\right)}$$

$$-\frac{\{1+bx-\emptyset e^{kx}cos^2\pi(x-t)-H_{pl}\}^{\left(2+\frac{1}{n}\right)}\{1+bx-\emptyset e^{kx}cos^2\pi(x-t)\}}{2^{\frac{1}{n}}\left(1+\frac{1}{n}\right)\left(2+\frac{1}{n}\right)}+\frac{\{1+bx-\emptyset e^{kx}cos^2\pi(x-t)-H_{pl}\}^{\left(3+\frac{1}{n}\right)}}{2^{\frac{1}{n}}\left(1+\frac{1}{n}\right)\left(2+\frac{1}{n}\right)\left(3+\frac{1}{n}\right)}$$

$$-\frac{\{1+bx-\emptyset e^{kx}cos^2\pi(x-t)-H_{pl}\}^{\left(1+\frac{1}{n}\right)}H_{pl}^2}{2^{\left(1+\frac{1}{n}\right)}\left(1+\frac{1}{n}\right)}, \quad (4.19)$$

and

$$T=\frac{\{1+bx-\emptyset e^{kx}cos^2\pi(x-t)-H_{pl}\}^{\frac{1}{n}}\left\{\begin{matrix}1-2\emptyset e^{kx}cos^2\pi(x-t)+\emptyset^2e^{2kx}cos^4\pi(x-t)+\\ b^2x^2+2bx-2bx\emptyset e^{kx}cos^2\pi(x-t)\end{matrix}\right\}\left\{\begin{matrix}b+\emptyset\, e^{kx}\sin 2\pi(x-t)\\ -\emptyset\, ke^{kx}cos^2\pi(x-t)\end{matrix}\right\}}{2^{\left(1+\frac{1}{n}\right)}\left(1+\frac{1}{n}\right)}. \quad (4.20)$$

The pressure gradient, in view of Eq. (4.18), is derived as

$$\frac{\partial p}{\partial x}\left|\frac{\partial p}{\partial x}\right|^{\left(\frac{1}{n}-1\right)}=\frac{1}{S}\left[\gamma\,(t)+\int_0^x\{-b\pi\emptyset\, e^{kx}\sin 2\pi(x-t)-\pi\emptyset\, e^{kx}\sin 2\pi(x-t)+\pi\emptyset^2\, e^{2kx}\sin 2\pi(x-t)\times cos^2\pi(x-t)\}dx\right], \quad (4.21)$$

where $\gamma\,(t)$ is an arbitrary function of t.

$$\frac{\partial p}{\partial x}=\frac{1}{S}\left[\gamma\,(t)+\int_0^x\{-b\pi\emptyset\, e^{kx}\sin 2\pi(x-t)-\pi\emptyset\, e^{kx}\sin 2\pi(x-t)+\pi\emptyset^2\, e^{2kx}\sin 2\pi(x-t)\,cos^2\pi(x-t)\}dx\right]\times$$

$$\left|\frac{1}{S}\left[\gamma\,(t)+\int_0^x\{-b\pi\emptyset\; e^{kx}\sin 2\pi(x-t)-\pi\emptyset\; e^{kx}\sin 2\pi(x-t)+\pi\emptyset^2\; e^{2kx}\sin 2\pi(x-t)\,cos^2\pi(x-t)\}\,dx\right]\right|^{n-1},$$

(4.22)

Integration of Eq. (4.22) from the inlet to the arbitrary axial point gives the general axial pressure along the length of the oesophagus as

$$p(x,t)-p(0,t)=\int_0^x\frac{1}{S}\left[\gamma\,(t)+\int_0^x\{-b\pi\emptyset\; e^{kx_1}\sin 2\pi(x_1-t)-\pi\emptyset\; e^{kx_1}\sin 2\pi(x_1-t)+\pi\emptyset^2\; e^{2kx_1}\sin 2\pi(x_1-t)\,cos^2\pi(x_1-t)\}dx_1\right]\left|\frac{1}{S}\left[\gamma\,(t)+\int_0^x\{-b\pi\emptyset\; e^{kx_1}\sin 2\pi(x_1-t)-\pi\emptyset\; e^{kx_1}\sin 2\pi(x_1-t)+\pi\emptyset^2\; e^{2kx_1}\sin 2\pi(x_1-t)\,cos^2\pi(x_1-t)\}dx_1\right]\right|^{n-1}dx,$$

(4.23)

so that the pressure difference between two ends of the oesophagus is given by

$$p(l,t)-p(0,t)=\int_0^l\frac{1}{S}\left[\gamma\,(t)+\int_0^x\{-b\pi\emptyset\; e^{kx_1}\sin 2\pi(x_1-t)-\pi\emptyset\; e^{kx_1}\sin 2\pi(x_1-t)+\pi\emptyset^2\; e^{2kx_1}\sin 2\pi(x_1-t)\,cos^2\pi(x_1-t)\}dx_1\right]\left|\frac{1}{S}\left[\gamma\,(t)+\int_0^x\{-b\pi\emptyset\; e^{kx_1}\sin 2\pi(x_1-t)-\pi\emptyset\; e^{kx_1}\sin 2\pi(x_1-t)+\pi\emptyset^2\; e^{2kx_1}\sin 2\pi(x_1-t)\,cos^2\pi(x_1-t)\}dx_1\right]\right|^{n-1}dx.$$

(4.24)

Now from Eq. (4.21), $\gamma\,(t)$is evaluated as

$$\gamma\,(t)=\left(\int_0^l\frac{1}{S}\,dx\right)^{-1}\left[\int_0^l\frac{\partial p}{\partial x}\left|\frac{\partial p}{\partial x}\right|^{\left(\frac{1}{n}-1\right)}dx-\int_0^l\frac{1}{S}\int_0^x\{-b\pi\emptyset\; e^{kx_1}\sin 2\pi(x_1-t)-\pi\emptyset\; e^{kx_1}\times\right.$$

$$\left.\sin 2\pi(x_1-t)+\pi\emptyset^2\; e^{2kx_1}\sin 2\pi(x_1-t)\,cos^2\pi(x_1-t)\}dx_1\,dx\right],$$

(4.25)

where S is given by expression (4.19). For $b=0,\ k=0,\ H_{pl}=0$ and $n=1$, Eqs. (4.22) – (4.25) reduce to corresponding equations derived by Li and Brasseur (1993) for Newtonian fluids.

4.3.1 Time averaged volume flow rate

The volume flow rate for single wave transport in the non-plug region is

$Q(x,t)=2\sigma\int_{H_{pl}}^{H}urdr$, where $\sigma=\frac{l}{\lambda}$.

Using Eq. (4.14), we have

$$Q(x,t)=-2\sigma\frac{\partial p}{\partial x}\left|\frac{\partial p}{\partial x}\right|^{\left(\frac{1}{n}-1\right)}S.$$

(4.26)

Now we define the following transformations between the wave and the laboratory frames in the non-dimensional form, where the parameters on the right side are in the laboratory frame and those on the left side are in the wave frame.

$$X = x - t,\ R = r,\ U(R,X) = u(r,x,t) - 1,\ V(R,X) = v(r,x,t), \tag{4.27}$$

and $q(X) = Q(x,t) - 1 + 2\emptyset e^{kx}cos^2\pi(x-t) - \emptyset^2 e^{2kx}cos^4\pi(x-t) - b^2x^2 - 2bx$
$+2bx\emptyset e^{kx}cos^2\pi(x-t) + H_{pl}^2$. (4.28)

The time-averaged-volume flow rate over a period in the laboratory frame for a single wave propagation, is defined by

$\bar{Q}(x) = \frac{1}{\sigma}\int_0^\sigma Q dt$,

which, in view of Eq. (4.28), yields

$$Q = \bar{Q} + 1 - 2\emptyset e^{kx}cos^2\pi(x-t) + \emptyset^2 e^{2kx}cos^4\pi(x-t) + b^2x^2 + 2bx$$

$$-2bx\emptyset e^{kx}cos^2\pi(x-t) - \frac{1}{\sigma}\int_0^\sigma \Big(1 - 2\emptyset e^{kx}cos^2\pi(x-t) + \emptyset^2 e^{2kx}cos^4\pi(x-t) + b^2x^2 +$$
$$2bx - 2bx\emptyset e^{kx}cos^2\pi(x-t)\Big)dt\ , \tag{4.29}$$

so that, from Eq. (4.26), we get pressure gradient in terms of time averaged volume flow rate as

$$\frac{\partial p}{\partial x} = \frac{1}{2^n\sigma^n} \times$$
$$\left[\frac{1}{s}\begin{Bmatrix} -1 + 2\emptyset e^{kx}cos^2\pi(x-t) - \emptyset^2 e^{2kx}cos^4\pi(x-t) - b^2x^2 - 2bx + 2bx\emptyset e^{kx}cos^2\pi(x-t) - \bar{Q} \\ +\frac{1}{\sigma}\int_0^\sigma \big(1 - 2\emptyset e^{kx}cos^2\pi(x-t) + \emptyset^2 e^{2kx}cos^4\pi(x-t) + b^2x^2 + 2bx - 2bx\emptyset e^{kx}cos^2\pi(x-t)\big)dt \end{Bmatrix}\right] \times$$
$$\left|\frac{1}{s}\begin{Bmatrix} -1 + 2\emptyset e^{kx}cos^2\pi(x-t) - \emptyset^2 e^{2kx}cos^4\pi(x-t) - b^2x^2 - 2bx + 2bx\emptyset e^{kx}cos^2\pi(x-t) - \bar{Q} \\ +\frac{1}{\sigma}\int_0^\sigma \big(1 - 2\emptyset e^{kx}cos^2\pi(x-t) + \emptyset^2 e^{2kx}cos^4\pi(x-t) + b^2x^2 + 2bx - 2bx\emptyset e^{kx}cos^2\pi(x-t)\big)dt \end{Bmatrix}\right|^{n-1}.$$
(4.30)

The pressure at a general axial point along the length of the oesophagus in terms of the time averaged volume flow rate is determined by integrating Eq. (4.30) from the inlet to the arbitrary axial point, and is given by

$$p(x,t) - p(0,t) = \frac{1}{2^n \sigma^n} \times$$

$$\int_0^x \left[\frac{1}{s} \left\{ \begin{matrix} -1 + 2\emptyset e^{kx} cos^2\pi(x-t) - \emptyset^2 e^{2kx} cos^4\pi(x-t) - b^2x^2 - 2bx + 2\text{bx}\emptyset e^{kx} cos^2\pi(x-t) - \bar{Q} \\ + \frac{1}{\sigma}\int_0^\sigma \left(1 - 2\emptyset e^{kx} cos^2\pi(x-t) + \emptyset^2 e^{2kx} cos^4\pi(x-t) + b^2x^2 + 2bx - 2\text{bx}\emptyset e^{kx} cos^2\pi(x-t)\right) dt \end{matrix} \right\} \right] \times$$

$$\left| \frac{1}{s} \left\{ \begin{matrix} -1 + 2\emptyset e^{kx} cos^2\pi(x-t) - \emptyset^2 e^{2kx} cos^4\pi(x-t) - b^2x^2 - 2bx + 2\text{bx}\emptyset e^{kx} cos^2\pi(x-t) - \bar{Q} \\ + \frac{1}{\sigma}\int_0^\sigma \left(1 - 2\emptyset e^{kx} cos^2\pi(x-t) + \emptyset^2 e^{2kx} cos^4\pi(x-t) + b^2x^2 + 2bx - 2\text{bx}\emptyset e^{kx} cos^2\pi(x-t)\right) dt \end{matrix} \right\} \right|^{n-1} dx, \quad (4.31)$$

where S is given by expression (4.19). For $H_{pl} = 0,\ k = 0$ and $b = 0$, Eq. (4.31) reduces to the corresponding equation for power-law fluids derived by Misra and Pandey (2001).

4.4 Numerical results and discussions

The intention behind this investigation is to derive the effect of sliding hiatus hernia on the swallowing of Herschel-Bulkley fluid with dilating peristaltic waves. This effect is discussed through two different cases. First, we consider that due to herniation oesophagus gets diverged near the distal end. Our second consideration is that at the distal end, some part of the oesophagus gets diverged and then converged.

Suppose that single bolus is swallowing in the oesophagus and oesophageal length is three times to the bolus, i.e. oesophagus can contain three boluses at a time in its length. Because, in practice, mostly only one bolus moves in the oesophagus when fluid is non-Newtonian. Pressure in the oesophagus is calculated numerically along its axis by setting zero pressure at the two ends of the oesophagus.

4.4.1 Divergence near the distal end of the oesophagus

We suppose that first two third length of the total oesophageal length is uniform in cross section and second one third is diverging. This diverged portion of the oesophagus is symbolically represented as $1 + bx$, where b is the slope of the tube wall. We consider six time instants $t = 0.0, 0.32, 0.79, 1.27, 1.72, 2.0$ for the temporal position of bolus. These time instants are randomly chosen.

4.4.1.1 Effect of the slope of the tube wall

The effect of the slope of the tube wall on pressure distribution is shown in Fig. 4.3. The pressure is measured at different time instants. We set $\emptyset = 0.6,\ k = 0.01,\ n = 1.1,\ H_{pl} = 0.01$ and b is varied in the range 0.0-0.30.

At $t = 0.0$ (Fig. 4.3(a)) it is observed that greater the slope of the tube wall, lower is the fall in pressure revealing a smaller requirement of pressure. The pressure distribution curves at $t = 0.32$ (Fig. 4.3(b)) show that the pressure rise, for diverging tube behind the bolus, is greater than that for uniform tube ($b = 0.0$) but pressure drop is lower than that for uniform tube. The pressure distribution curves show the similar trends at $t = 0.79$ (Fig. 4.3(c)) and $t = 1.27$ (Fig. 4.3(d)) as the previous. At $t = 1.72$ (Fig. 4.3(e)) and $t = 2.0$ (Fig. 4.3(f)), when bolus is situated within the diverged part of the oesophagus, pressure rises here but is less for the diverging tube in comparison to the uniform tube. Comparison of plots at $t = 0.0$ and $t = 2.0$ (Fig. 4.3, corresponding to $b = 0.15,\ 0.30$) show that the difference between the maximum and the minimum pressures becomes smaller when the tube diverges. In other words, for diverging tube the upper oesophageal sphincter pressure may be larger than that of the lower oesophageal sphincter pressure. This substantiates the experimental observation of Kahrilas et al. (1999).

When bolus is about to enter in stomach, pressure rises and falls less in a diverging tube than that in uniform tube. Therefore, the pressure requirement to deliver the bolus in stomach is smaller for diverging oesophagus than that of uniform. The interesting observation is that although tube diverges near the end only, its impact is seen on the pressure distribution right from the beginning of the oesophagus.

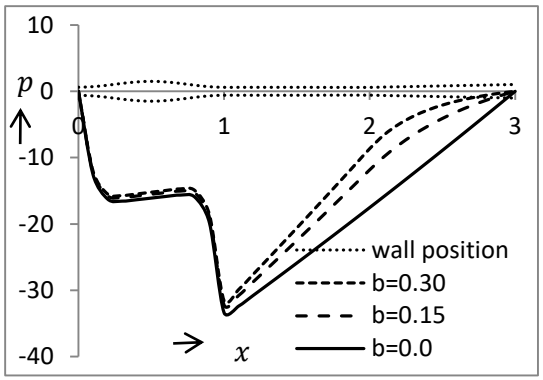

(a) $t = 0.0$

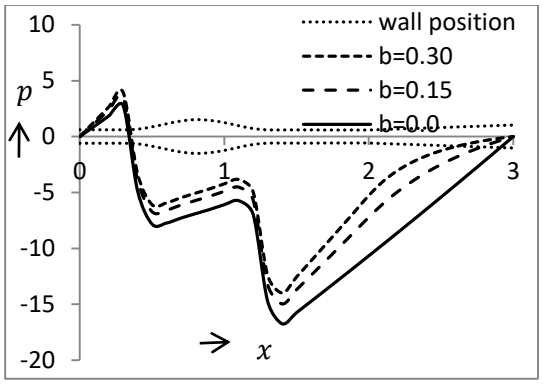

(b) $t = 0.32$

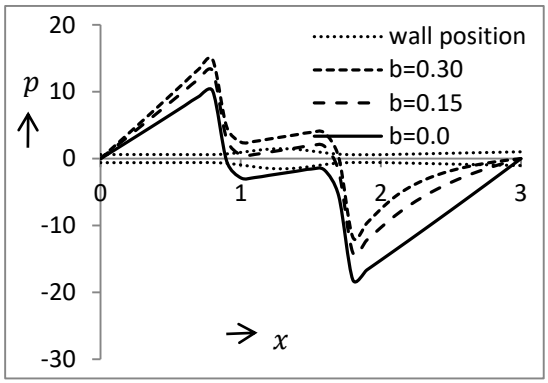

(c) $t = 0.79$

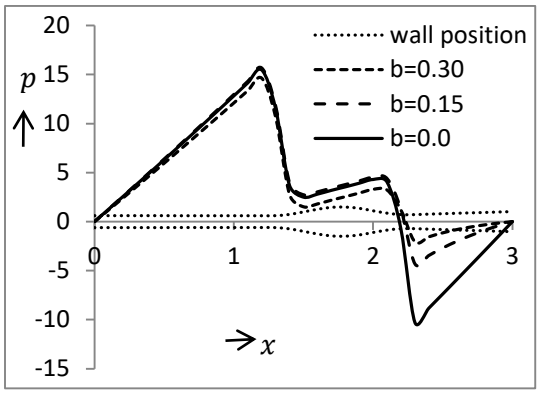

(d) $t = 0.27$

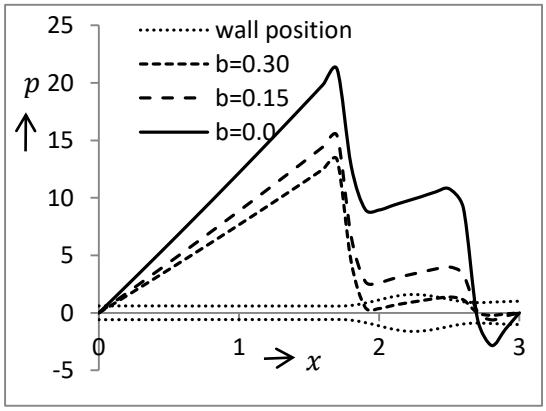

(e) $t = 1.72$

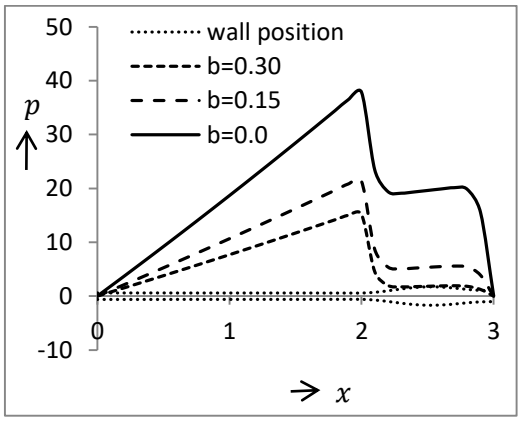

(f) $t = 2.0$

Fig. 4.3(a-f) *Pressure variation along the length of oesophagus at different instants showing the effect of tube wall slop* b *when tube diverges at distal end. Other parameters are taken as* $\emptyset = 0.6,\ H_{pl} = 0.01,\ k = 0.01,\ n = 1.1.$

The effect of the slope of the tube wall on pressure rise over one wavelength vs. time-averaged flow rate is shown in Fig. 4.4, which is based on Eq. (4.31). We set $\emptyset = 0.6,\ k = 0.01,\ n = 1.1,\ H_{pl} = 0.01, t = 0$ and vary b in the range 0.0-0.2. We observe that the greater the slope of the tube wall, the greater is the rise in the pressure per wavelength. It is also observed that below a fixed $\bar{Q}$, pressure rise over one wavelength is positive and above that it is negative. Negative pressure rise enhances the flow.

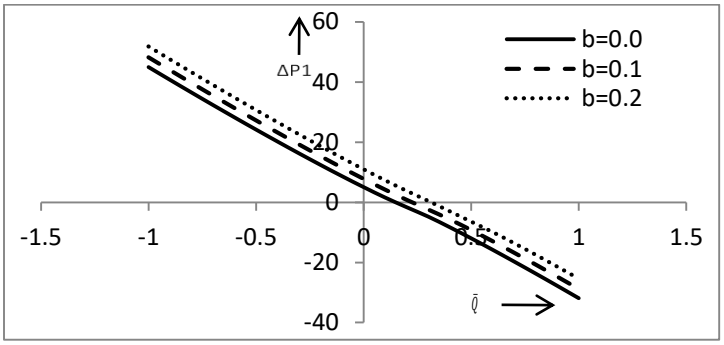

Fig. 4.4 *Pressure rise over one wavelength vs. time-averaged flow rate showing the effect of tube wall slop b when tube diverges at distal end. Other parameters are taken as* $\emptyset = 0.6,\ H_{pl} = 0.01,\ k = 0.01, t = 0,\ n = 1.1.$

4.4.1.2 Effect of dilating wave amplitude

Dilating wave amplitude effect on the flow dynamics is demonstrated in Fig. 4.5. For investigation, we set $\emptyset = 0.6,\ H_{pl} = 0.01,\ n = 1.1,\ b = 0.3$ and assume three values of dilation parameter $k = 0.0, 0.02, 0.04$. Pressure curves corresponding to $t = 0.0 - 2.0$ (Fig. 4.5) reveal that greater the dilation parameter, higher the pressure gradient. Comparison of plots at $t = 0.0$ and $t = 2.0$ (Fig. 4.5) show that lower oesophageal sphincter pressure may be lower than that of upper oesophageal sphincter pressure which is unlike the finding of Pandey et al. (2017) that due to dilating wave amplitude lower oesophageal sphincter pressure is greater than that of upper oesophageal sphincter pressure in uniform tube.

Impact of the dilating wave amplitude on the pressure rise over one wavelength vs. the time-averaged flow rate is shown in Fig. 4.6. We set $\emptyset = 0.6,\ b = 0.1,\ n = 1.1,\ H_{pl} =$

$0.01, t = 0$ and $k = 0.0, 0.02, 0.04$. We observe that the greater the slope of the tube wall, the greater is the rise in the pressure per wavelength. It is observed that the pressure rise over one wavelength increases with the dilation parameter.

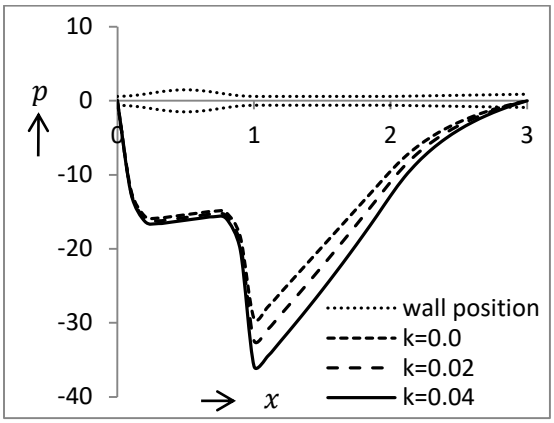

(a) $t = 0.0$

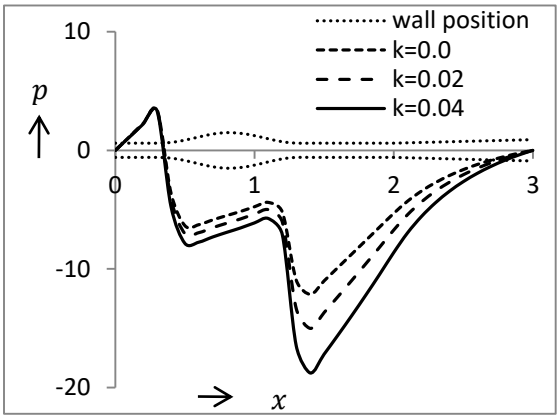

(b) $t = 0.32$

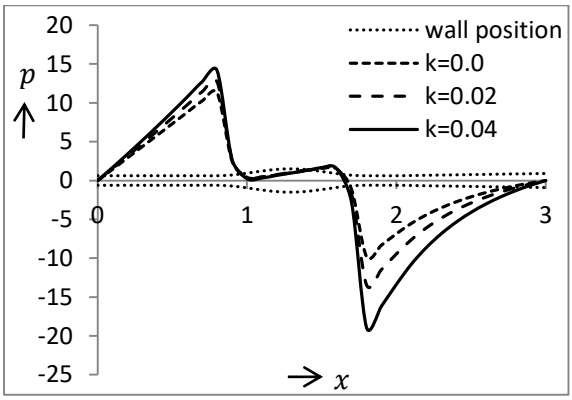

(c) $t = 0.79$

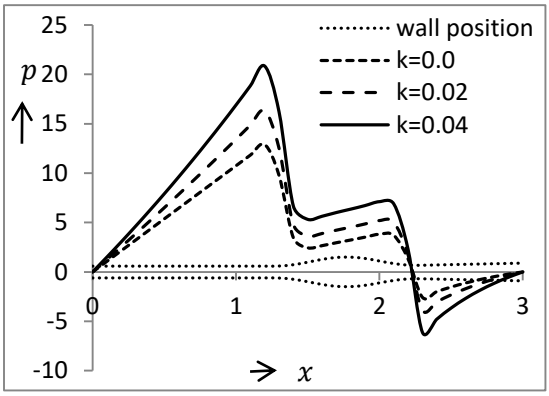

(d) $t = 1.27$

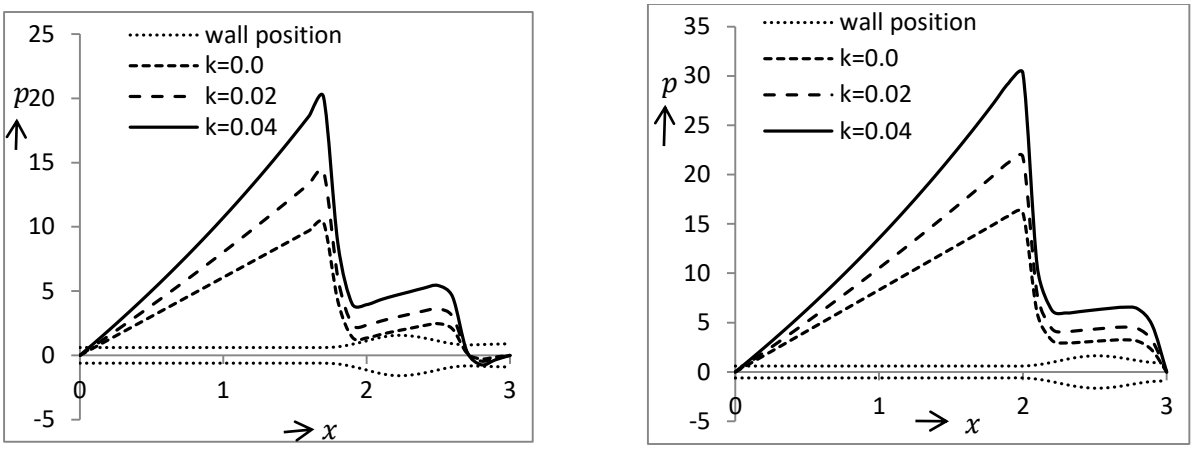

(e) $t = 1.72$ (f) $t = 2.0$

Fig. 4.5(a-f) *Pressure variation along the length of oesophagus at different instants showing the effect of dilation parameter k when tube diverges at distal end. Other parameters are taken as* $\emptyset = 0.6,\ H_{pl} = 0.01,\ n = 1.1,\ b = 0.3.$

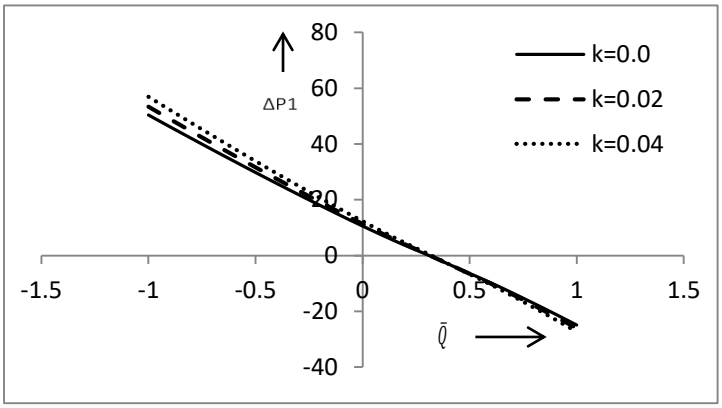

Fig. 4.6 *Pressure rise over one wavelength vs. averaged flow rate showing the effect of dilation parameter, k, when tube diverges at distal end. Other parameters are taken as* $\emptyset = 0.6,\ H_{pl} = 0.01,\ b = 0.2,\ t = 0,\ n = 1.1.$

4.4.1.3 Effect of flow behaviour index

Herschel-Bulkley fluid is a general type of fluid which requires a finite stress, known as yield stress and nonlinear effective viscosity coefficient. For investigation, we assume three values $n = 0.9, 1.0, 1.1$. The three values represent three different types of fluids, namely, pseudo plastic, Newtonian and dilatants respectively if the yield stress is considered to be zero. The

dilation parameter, the plug flow region and the slope of the tube wall are fixed as $k = 0.01$, $H_{pl} = 0.01$ and $b = 0.3$ respectively for investigating the impact of flow behaviour index n (Fig. 4.7). It is observed that pressure increases with increasing flow behaviour index.

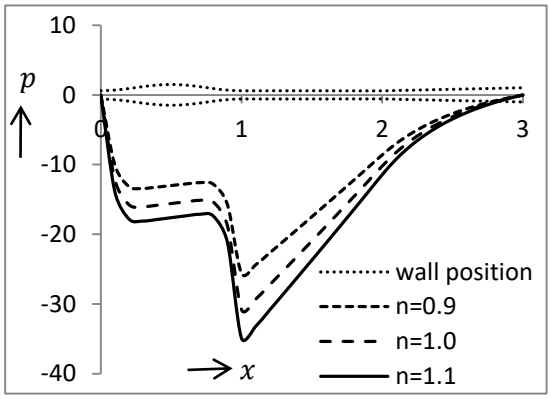

(a) $t = 0.0$

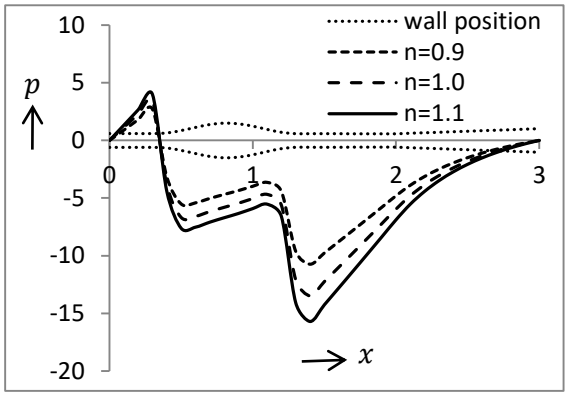

(b) $t = 0.32$

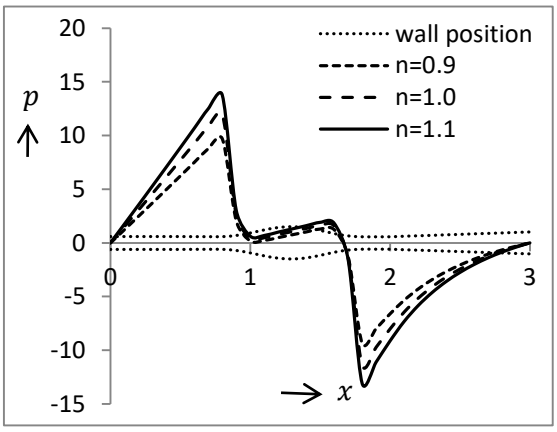

(c) $t = 0.79$

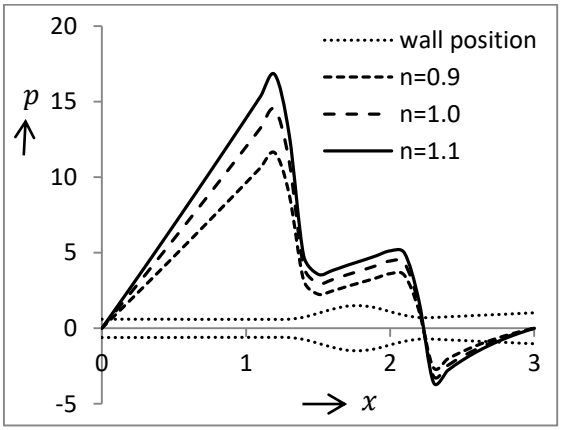

(d) $t = 1.27$

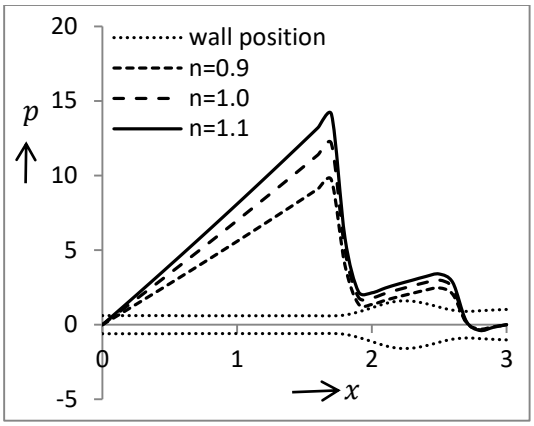

(e) $t = 1.72$

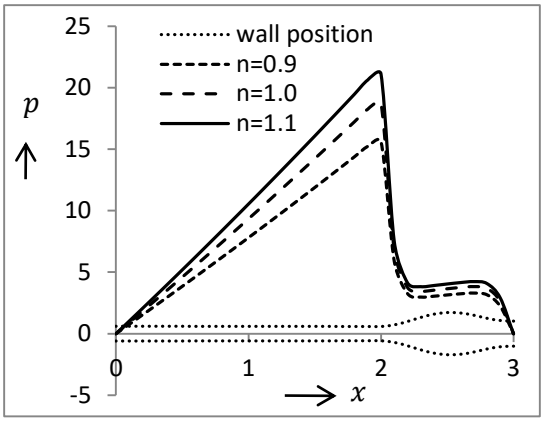

(f) $t = 2.0$

Fig. 4.7(a-f) *Pressure variation along the length of oesophagus at different instants showing the effect of flow behaviour index* n *when tube diverges at distal end. Other parameters are taken as* $\emptyset = 0.6,\ H_{pl} = 0.01,\ k = 0.01,\ b = 0.3$.

4.4.2 Divergence and then convergence near the distal end of the oesophagus

Now, our second consideration is that near the distal end, a part of the oesophagus diverges and then converges. For the sake of convenience, we consider that first one third length of oesophagus is uniform in cross sectional area, second one third length diverges and third one third length converges. The degrees of divergence and convergence are retained as the same with respect to the uniformly kept cross sectional area of the oesophageal wall. The time instants are considered the same as the previous case for the temporal position of the bolus.

4.4.2.1 Effect of the slope of the tube wall

The diagrams in Figs. 4.8(a)-(f) exhibit variation of pressure along the axis at different time instants when the oesophagus has diverged and converged near its end at different rates $b = 0.0, 0.2, 0.4$. Rest of the parameters are set as $\emptyset = 0.6,\ k = 0.01,\ n = 1.1,\ H_{pl} = 0.01$.

In Figs. 4.8(a)-(f), as in the previous case, we observe that pressure is affected right from the beginning, although tube diverges and then converges near the distal end. In Fig. 4.8(a) it is observed that unlike diverging region, more pressure is required to transport fluid when it converges.

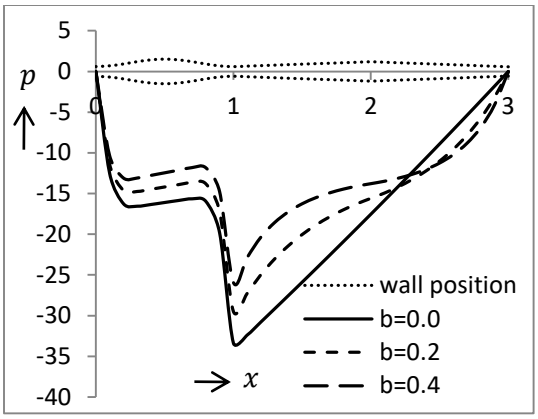

(a) $t = 0.0$

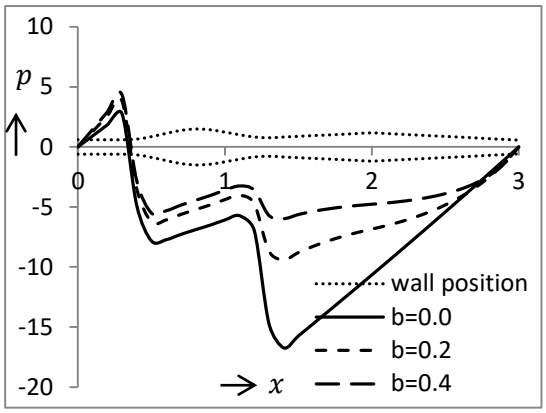

(b) $t = 0.32$

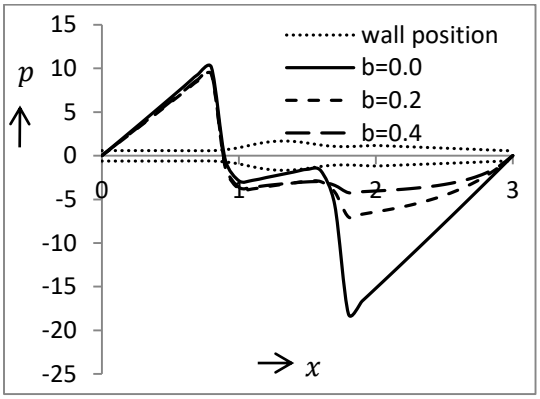

(c) $t = 0.79$

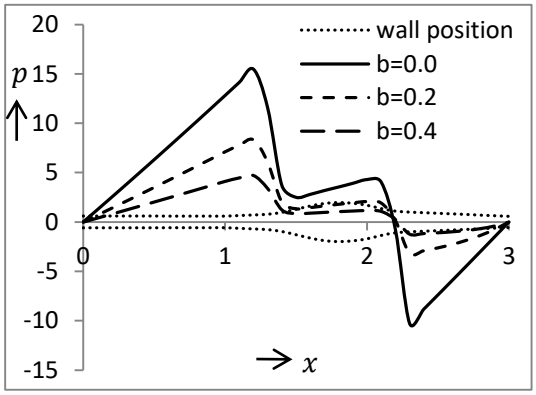

(d) $t = 1.27$

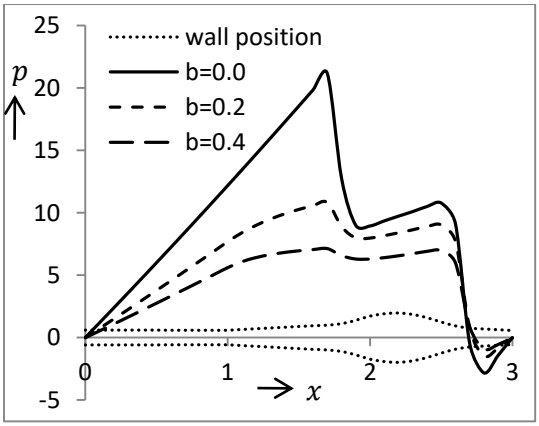

(e) $t = 1.72$

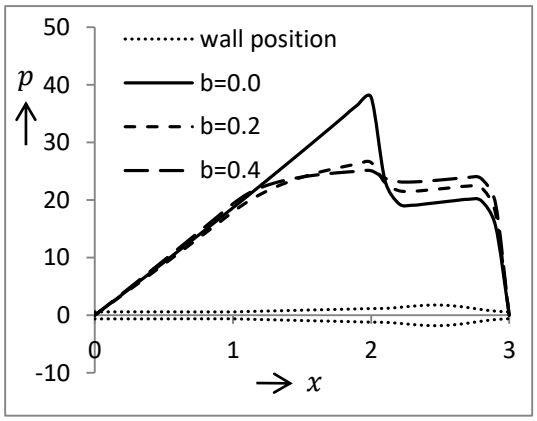

(f) $t = 2.0$

Fig. 4.8(a-f) *Pressure variation along the length of oesophagus at different instants showing the effect of tube wall slop b when tube diverges and then converges at distal end. Other parameters are taken as* $\emptyset = 0.6,\ H_{pl} = 0.01,\ k = 0.01,\ n = 1.1.$

4.5 Conclusions

Peristaltic flow of Herschel-Bulkley fluid in a circular cylindrical tube of variable cross section models swallowing in the oesophagus. We conclude that the difference between the maximum and the minimum pressures becomes smaller when the tube diverges. In other words, for the diverging tube the upper oesophageal sphincter pressure may be larger than that of lower oesophageal sphincter pressure. Kahrilas et al. (1999) in their experiment with swallowing of patients suffering from sliding hiatus hernia observed lower pressure in the distal oesophagus. This validates our theoretical finding. When the bolus is nearing the cardiac sphincter, pressure-rise and pressure-drop are less in a diverging tube than that in a uniform tube. Therefore, the pressure requirement to deliver bolus in stomach is less if oesophagus diverges. Probably, this is the reason why patient is ignorant of sliding hiatus hernia. However, some more symptoms such as heartburn and regurgitation are probable. Since any such ignorance may lead to a more dangerous situation, i.e. para-oesophageal hiatal herniation, it is therefore suggested that medical intervention should start at this stage itself although the patient feels no pain initially. This easy swallowing may aggravate the situation. Apart from this, whenever there is rise of pressure in the abdomen, vomiting may easily occur. Another interesting observation is that although tube diverges near the end only, its impact is seen on the pressure distribution right from the beginning of swallowing in the oesophagus.